

We are IntechOpen, the world's leading publisher of Open Access books Built by scientists, for scientists

6,900

Open access books available

186,000

International authors and editors

200M

Downloads

Our authors are among the

154

Countries delivered to

TOP 1%

most cited scientists

12.2%

Contributors from top 500 universities



WEB OF SCIENCE™

Selection of our books indexed in the Book Citation Index
in Web of Science™ Core Collection (BKCI)

Interested in publishing with us?
Contact book.department@intechopen.com

Numbers displayed above are based on latest data collected.
For more information visit www.intechopen.com



Formation and Transformation of Typical Pollutant from MSW by Hydrothermal Carbonization towards Biofuel Hydrochar Production

Wentao Jiao, Nana Peng and Zhengang Liu

Abstract

An unprecedented increase in municipal solid waste (MSW) is increasingly attractive in response to waste-to-energy. MSW pretreatment is an essential step due to the inherent properties of MSW. Hydrothermal carbonization (HTC) offers an efficient approach for converting MSW into carbonaceous hydrochars. In this chapter, the formation and transformation of heavy metals and polycyclic aromatic hydrocarbons (PAHs) during HTC of MSW were determined. The results indicated that HTC can homogenize the density and size of MSW and also increase carbon content. Moreover, the concentrations of heavy metals in the leachates of the hydrochars were lower than the United States Environmental Protection Agency (US EPA) maximum limits. Compared to MSW, the concentrations of Cr, Cd, Hg, and Zn in the hydrochars were low and the concentrations of Pb, As, Ni, and Cu were high. The concentrations of PAHs in the hydrochars increased with increasing temperature in the range of 1298.71–177698.20 $\mu\text{g}/\text{kg}$, which were much higher than that in MSW, except for H-160. The dominant PAH rings in MSW and the hydrochars were four-ring PAHs and three-ring PAHs, respectively. These findings suggest that 180°C is an appropriate hydrothermal temperature to reduce heavy metals and the toxicity PAHs of MSW.

Keywords: biomass, waste-to-energy, fuel quality, heavy metals, polycyclic aromatic hydrocarbons, hydrochar

1. Introduction

At present, municipal solid waste (MSW) generated in daily life is the major waste in the urban management, which consists of food waste, plastics, paper, garden waste, textiles, stone, glass, etc. [1]. An unprecedented increase in the amount of MSW is observed in all over the world, especially for the populous development countries, such as India and China due to the population growth, rapid urbanization, and industrialization [2, 3]. It is reported that about 1.70–1.90 billion metric tons per year of MSW is produced in the world [4]. In China, the MSW delivering quantity had grown to 0.20 billion metric tons in 2016 [5]. It is estimated that China

will generate about 0.50 billion metric tons at 2025 and contribute nearly 25% to total world's MSW amount [6]. Therefore, the disposal of MSW has been and will continue to be an urgent and major issue. Landfill, incineration, and composting are commonly applied for the treatment of MSW [7–9]. Among those methods, landfill is the most common disposal method of MSW in China due to the cost-effective and low requirements of both separation and technique. However, the landfill suffers from many problems, such as serious secondary pollution from the leachate, the increasing cost of land acquirement due to the increase development of population and urbanization, and so on [10]. The incineration of MSW can achieve effectively energy recovery, reduce waste volume by 90% and waste weight by 70%, and decrease the toxicity [11]. Additionally, an increase in the combustible components of MSW such as plastics and papers improves the combustibility of MSW. On the other hand, the quick depletion of fossil fuels and worldwide environmental pollution promote the development of sustainable energy obtained from renewable resources like MSW. In view of those advantages, incineration as an economically feasible way for the effective energy recovery from MSW has been paid great attention in recent years. For example, in the last 10 years, an increase in the incineration treatment rate of MSW in China is observed in the range of 14.52–37.51% [5]. But the specific properties of MSW are the major drawbacks to employ it as an energy feedstock for incineration, such as the high moisture and oxygen contents, low carbon content, and the heterogeneity. To overcome these problems, pretreatment technology is need to homogenize raw MSW and improve its fuel property.

Hydrothermal carbonization (HTC), also known as hydrothermal upgrading, wet torrefaction, or coalification, is a wet and moderate temperature (180–350°C) process in an autogenous or elevated pressures reactor [12–15]. Water is a necessary component and plays an important role during HTC, which exists as a hot, expanded liquid or possibly supercritical state to participate in the reaction as reactants or contributes to the changes in the free energy of activation [13, 16]. A series of hydrolysis, decarboxylation, dehydration, and condensation reactions occur during HTC resulting in carbonaceous solid product known as the hydrochar, aqueous, and gases [17]. The distributions and characteristics of the products are strongly affected by the HTC conditions, and many studies present reaction temperature plays the most important role [14, 18]. Compared to other dry carbonization processes (such as gasification and pyrolysis), HTC do not need to spend extra energy on the drying process of raw biomass. On the other hand, HTC takes place in low temperature and has high conversion efficiency. For example, the solid products produced from HTC and pyrolysis were determined and compared based on the fuel qualities, and the results showed that the hydrochar obtained from HTC had higher energy density and thermal efficiency and lower pollutant emissions than that obtained from pyrolysis [19, 20], confirming that HTC can proceed with the same level of conversion efficiency as higher-temperature processes of dry carbonization [21, 22].

The first experiment about HTC was used in cellulose (which is known to pure material) to produce carbonaceous materials in 1913 [21, 23], and then early reviews were published in 1993 and 1994 [24, 25]. To date, the feedstocks supplied for HTC rang from pure materials to more complex biomass, such as agriculture waste [26–28], manure [29], alga [30], and so on [18, 31]. Recently, the acid or basic solution can also be applied into the feedwater in order to remove the metals and increase the hydrochar yield solution [26, 32, 33]. The existing literature covers a wide range of studies on HTC of biomass and has been proved that HTC as a novel thermal pretreatment process is a promising and viable method to homogenize the biomass, increase the carbon content, decrease moisture content, and increase grindability [21, 31]. Generally, the potential to use the hydrochar has concentrated on the alternative fuel for energy supply and additive agent for soil amendment.

With the application of the hydrochars, environmental issues should be considered, such as the pollution risk of heavy metals and the emissions of polycyclic aromatic hydrocarbons (PAHs).

Biomass contains various metals such as light metals and heavy metals during the metabolic demands for the growth process. However, those metals usually remain in the ash during the combustion because of their high melting point, leading to the slagging/fouling and the negative impact on the environment. Several investigations have been published about the removing of light metals during HTC of lignocellulosic biomass [20, 34]. The results show that light metals can be easily removed from raw biomass during HTC due to the water solubility properties [20]. In contrast to light metals, heavy metals exhibit the different chemical forms and is expected to result in the different remove rates. Additionally, considering the potential risk to the environment and health, heavy metals like chromium (Cr), cadmium (Cd), zinc (Zn), copper (Cu), nickel (Ni), arsenic (As), mercury (Hg), and lead (Pb) have been the worldwide concern [35]. However, the transformation of heavy metals during HTC process has not yet been studied in detail, especially for the MSW.

PAHs are known as persistent organic pollutants due to the long-range transport potential and the effect of mutagenicity, teratogenicity, and carcinogenicity [36]. Many studies provide the evidence that the environmental levels of PAHs have a significant inhibitory effect on human health and the growth of animals and plants [37, 38]. PAHs generated from the combustion or pyrolysis of solid fuels, such as MSW with the human industrialization, are widespread pollutants in the environment [36, 39]. Moreover, stricter standards on PAHs in recent years must be established to satisfy the social needs. Consequently, numerous researches on the decomposition and formation of PAHs have been reported in literature in order to control PAH emission from combustion or pyrolysis of coal [40], biomass [41], and so on [39, 42]. It is noteworthy that free PAHs are referred to the PAHs contained in the macromolecular structure of the feedstocks, which are easily able to emit into the environment [43]. Compared to PAHs generated from combustion or pyrolysis, limited investigations are known on free PAHs in coal [44], MSW ashes [45], and biochar obtained of biomass [46]. However, to our best knowledge, no study clearly has been done to investigate the free PAHs in MSW and corresponding hydrochars.

With the widespread application of the hydrochar, it is essential to investigate the formation and transformation of heavy metals and PAHs during HTC of MSW. Considering the significant effect of hydrothermal temperature, the concentrations of heavy metals and PAHs in MSW and corresponding hydrochars were determined in this chapter to evaluate the effect of HTC on the transformation of heavy metal and PAHs.

2. Preparation and characterization of biofuel hydrochar

Organic components of MSW were investigated in the present study, which was comprised of food waste (64.93 wt.%), plastics (15.07 wt.%), paper (12.94 wt.%), wood waste (1.48 wt.%), and textiles (3.11 wt.%) [10]. HTC of MSW was undertaken using a Morey-type reaction vessel that included a laboratory 50-mL Teflon reaction vessel and an SUS steel pressure vessel [47]. Briefly, the MSW and de-ionized water (a mass ratio of 1:3) was mixed using a stirrer and was fed to the vessel. Furthermore, the vessel was sealed and heated to the desired temperature using an oven. Experiments were conducted at different temperatures (160, 180, 200, 220, 240, and 260°C) for 10 h. After the reaction time was completed and the reactor had cooled down to room temperature, the solid product, called the hydrochar, was collected by vacuum filtration and dried at 50°C for 24 h before use. The hydrochar

yield was calculated as the mass ratio of the hydrochar and the MSW. There are three replicates for each hydrochar. H-x represented the hydrochar produced at some hydrothermal temperature, where x was the centigrade temperature.

The inductively coupled plasma-optical emission spectroscopy (ICP-OES, USA) was used to determine the concentrations of heavy metals, except for Hg. About 0.1 g of MSW or the hydrochar was digested in Teflon reactor by the mixed acids (4 mL 65% HNO₃, 4 mL 30% H₂O₂, 2 mL 70% HClO₄, and 4 mL 48% HF). The reactor was sealed and operated at 170°C for 12 h in order to dissolve the sample. After the reactor was cooled to the ambient temperature, the liquid solution was transferred to FTFE beaker, which was placed on electric hot plate to remove the moisture. Furthermore, the residual was re-dissolved using 1:1 v/v ratio of HNO₃ to the desired concentration and filtered with the glass fiber filter for ICP-OES analysis.

The concentration of Hg was analyzed on the cold atomic fluorescence mercury meter after total dissolution. For each experiment, a sample of approximately 0.2 g and mixed acids (4 M HCl and 2 M HNO₃) were sent to the glass tube and heated to 95°C for 1.5 h. Furthermore, 10 mL 0.05% K₂Cr₂O₇ (diluted by 5% HNO₃) was added to the mixed solution after cooling down to ambient temperature and then diluted to the desired concentration. The solution was filtered and analyzed by the cold atomic fluorescence mercury meter.

The toxicity characteristic leaching procedure (TCLP) was carried out according to the ASTM method 1311 in order to elucidate the potential mobility of heavy metals in the hydrochars [48]. 0.5 g of dried hydrochar was weighed and dissolved in 10 mL of TCLP extraction fluid. After rotated for 18 h, the solution was filtered through glass fiber (0.6–0.8 μm) and acidified with 1 M HNO₃ to pH 2 for ICP-OES analysis.

To determine the concentrations of PAHs, 0.5 g of the sample was Soxhlet extracted in dichloromethane (DCM) as the extraction solvent for 24 h. The extract was concentrated by a rotary evaporator at temperature around 38°C. A total of 15 mL of n-hexane was added and reconcentrated to 1 mL for solvent exchange [49]. The silica column was used for cleanup, which filled with silica gel particles (100–200 mesh), anhydrous sodium sulfate, and aluminum oxide from the bottom to the top. The extract was transferred to the silica column and eluted with n-hexane and a mixed solvent (n-hexane and DCM 7:3 (v/v), 70 mL). The fraction in the mixed solvent was solvent-exchange to n-hexane, concentrated to nearly dryness with a gentle blow of N₂, and diluted to 1 mL for analysis. The fraction was analyzed on a gas chromatograph-mass spectrometer (GC-MS, GC model Agilent 6890 and MS model 5793, USA) equipped with a DB-5MS column (30 m × 0.25 mm i.d., 0.25 μm film thickness). The GC oven was set to an initial temperature of 50°C, held in 2 min, and heated to 300°C at the rate of 6°C/min with final hold time at 300°C of 5 min.

An external standard calibration was used for the quantification of 16 priority PAHs. The examined 16 priority PAHs were shown in **Table 1**. Toxic equivalent factor (TEF) is used to take BaP as a toxic benchmark, and the corresponding TEF of individual PAHs can be found elsewhere [50]. The surrogate standards including naphthalene-d₈, perylene-d₁₂, acenaphthene-d₁₀, and phenanthrene-d₁₀ were applied for determining the recovery rate of PAHs. The recoveries for surrogate standards were in the range of 71.45–124.06%.

The surface morphology of the hydrochars was investigated using a field emission scanning electron microscopy (FESEM) model JSM-7500F. The sample dried at 105°C for 24 h was kept onto a carbon tape, coated with Au, and then placed under high vacuum condition. For each sample, at least five different sites were taken to increase the accuracy.

Ring number	Individual PAHs	Abbreviations	TEF
2	Napthalene	Nap	0.001
3	Acenaphthylene	Acy	0.001
	Acenaphthene	Ace	0.001
	Fluorene	Flu	0.001
	Phenanthrene	Phe	0.001
	Anthracene	Ant	0.010
4	Fluoranthene	Fla	0.001
	Pyrene	Pyr	0.001
	Benz[a]anthracene	BaA	0.100
	Chrysen	Chr	0.010
5	Benzo[b]fluoranthene	BbF	0.100
	Benzo[k]fluoranthene	BkF	0.100
	Benzo[a]pyrene	BaP	1.000
	Dibenz[ah]anthracene	DaA	1.000
6	Indeno[1,2,3-c,d]pyrene	IcP	0.100
	Benzo[ghi]perylene	BgP	0.010

Table 1.
 The 16 priority PAHs and corresponding TEF value.

3. Characteristics of MSW and biofuel hydrochars

3.1 Physicochemical properties of biofuel hydrochar

The yields of the hydrochars obtained from MSW during HTC are summarized in **Figure 1**. As expected, the yields of hydrochars in the range of 37.68–70.37% gradually decreased with increasing hydrothermal temperature from 160 to 260°C. A significant decrease of hydrochar yield was observed with the increase from 160 to 200°C. The hydrothermal temperature had no obvious effect on the hydrochar yield when the temperature was higher than 200°C. The quickest decrease of hydrochar yield was observed again at hydrothermal temperature from 240 to 260°C. The highest decrease of hydrochar yield at low temperature can be linked with easy decomposition of the protein, carbohydrate, and lipid in MSW. Furthermore, the decomposition of the char effectively caused the obvious decrease of hydrochar yield when the temperature was above 240°C.

Table 2 showed the ultimate analysis, the ratios of H/C and O/C, and HHV of MSW and corresponding hydrochars. The carbon content and oxygen content of MSW were 42.13 and 49.10%, respectively. As expected, compared to MSW, the carbon contents of the hydrochars were higher than that of MSW, except for H-160, while the contents of hydrogen, sulfur, nitrogen, and oxygen were roughly lower. It was noteworthy that compared to MSW, the H/C and O/C ratios of the hydrochars were observed to be low, indicating that the hydrochars had higher heating values and reduced energy loss during the combustion, which was consistent with the previous studies [51, 52]. This may be explained by the decrease of low-energy H–C and O–C bonds and the increase of high-energy C–C bonds [51]. The higher heating values (HHV) of MSW and corresponding hydrochars were investigated, and the results showed that the HHV of the hydrochars (in the range of 16.06–31.76 MJ/kg) almost increased with increasing

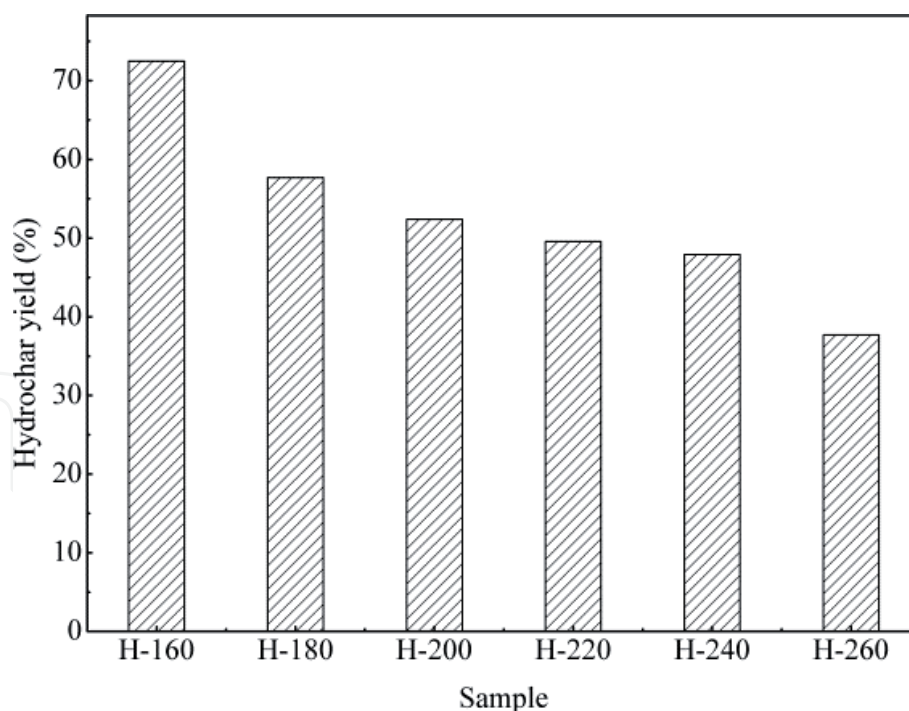


Figure 1.
The yields of the hydrochars obtained from MSW during HTC.

		MSW	H-160	H-180	H-200	H-220	H-240	H-260
Ultimate analysis (db, %)	C	42.13	41.92	49.3	65.15	73.88	67.16	75.71
	H	6.93	5.73	5.64	5.98	5.96	5.84	6.06
	S	0.29	0.28	0.26	0.26	0.20	0.25	0.17
	N	1.55	0.94	1.02	1.21	1.13	1.27	1.23
	O ^a	49.10	51.13	43.78	27.40	18.83	25.48	18.06
H/C		1.97	1.64	1.37	1.10	0.97	1.04	0.96
O/C		0.87	0.91	0.67	0.31	0.19	0.28	0.17
HHV (MJ/kg)		17.73	16.06	20.27	26.91	30.79	27.64	31.76

^aBy difference.

Table 2.
Ultimate analysis, the ratios of H/C and O/C, and HHV of MSW and corresponding hydrochars.

temperature, which were higher than that of MSW (17.73 MJ/kg), except for H-160. It is reported that the HHV of the solid fuel must be higher than 20 MJ/kg in order to ensure autothermal combustion [53]. In the present study, the HHV of the hydrochars exceeded 20 MJ/kg, except for H-160. The above results demonstrate that the hydrochar obtained from MSW above 160°C can be considered as a promising solid fuel.

3.2 The surface morphology of biofuel hydrochar

Figure 2 showed the appearances of MSW and the hydrochars obtained from HTC of MSW. It should be noticed that the individual components of MSW and H-160 were still observed. When the hydrothermal temperature was higher than 180°C, the hydrochars were homogenized and grinded into particles, indicating that HTC was an effective method for homogenizing the MSW.

The effect of hydrothermal temperature on the morphology characteristic of the MSW was shown in **Figure 3**. It was found that the hydrochar had a rough surface.

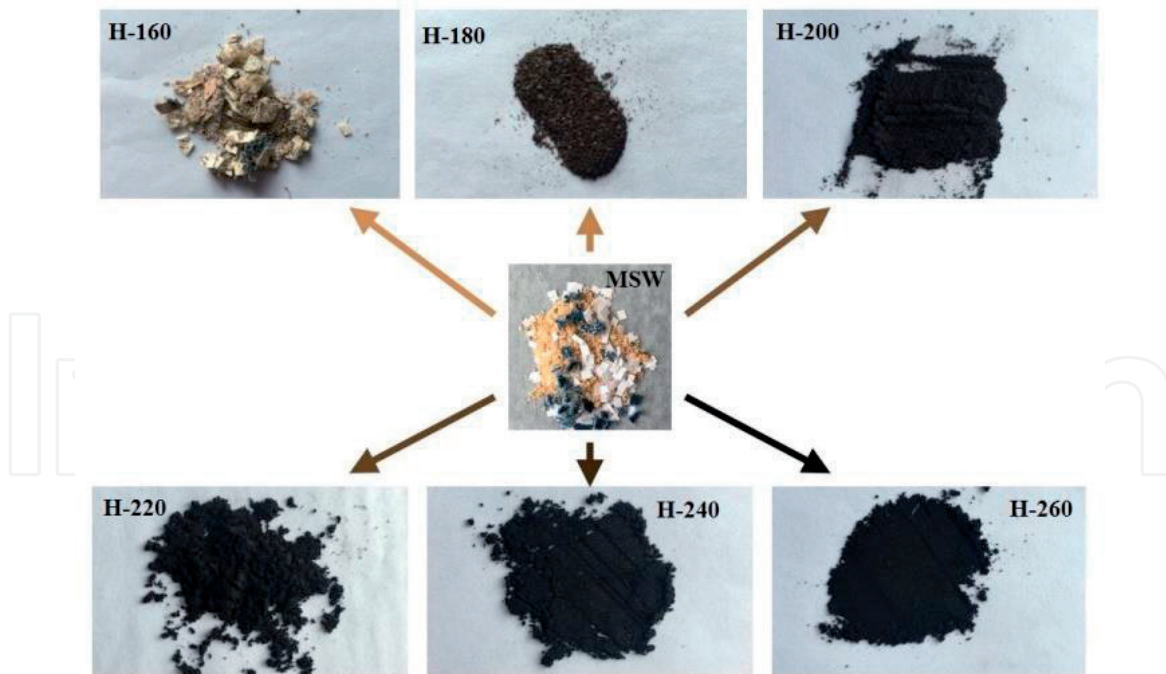


Figure 2.
The appearances of MSW and corresponding hydrochars.

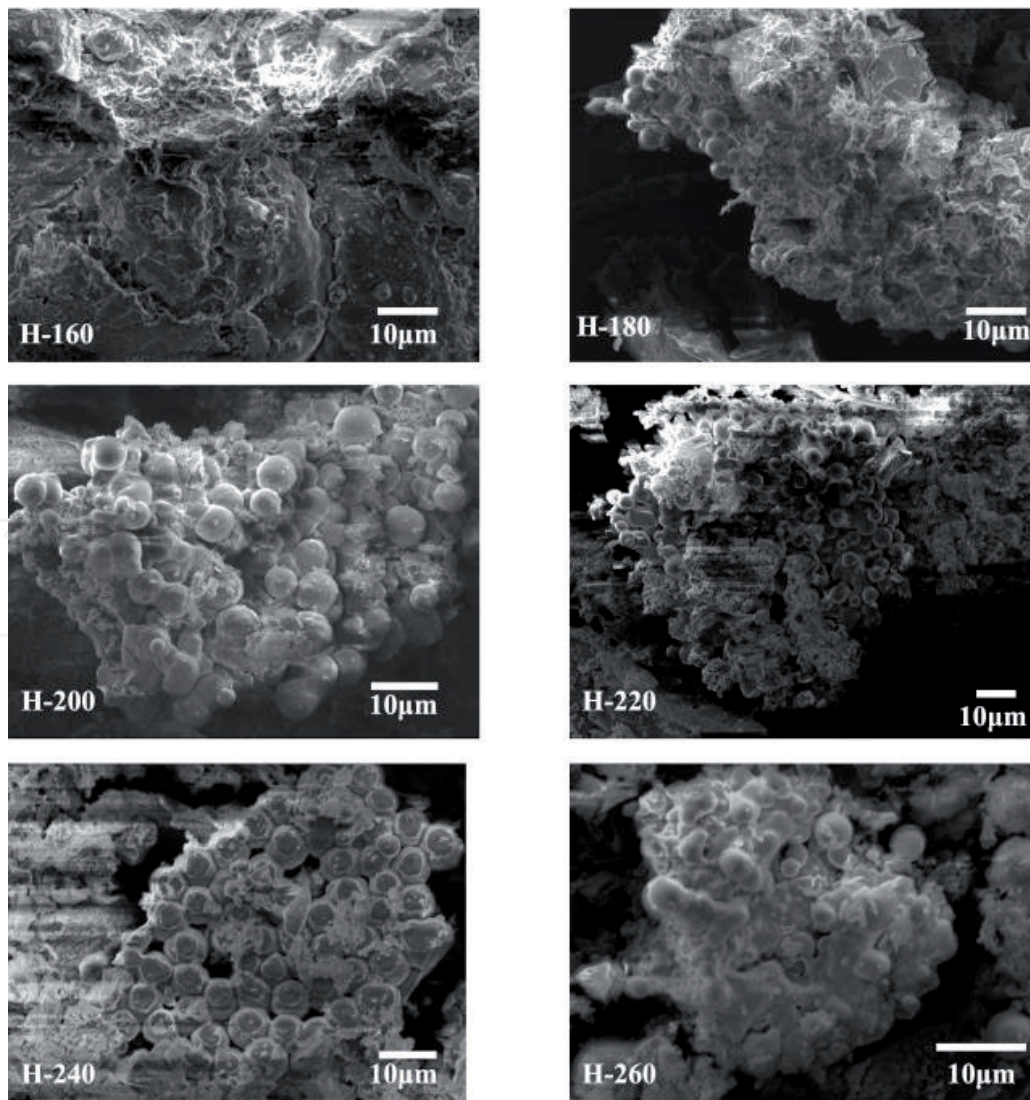


Figure 3.
SEM of the hydrochars obtained from MSW.

With the increasing hydrothermal temperature from 160 to 240°C, the microspheres appeared, and the number of those microspheres increased. The formation of microsphere number increased due to the decomposition or carbonization of MSW. Protein, cellulose, and other components in MSW firstly decompose into small fragments and then are melted and carbonized with the rise of hydrothermal temperature, resulting in the formation of carbon microspheres [54]. When the temperature was higher, however, the microspheres were damaged.

4. The transformation of heavy metals during HTC of MSW

Table 3 presented the mobility of heavy metals in the hydrochars using the TCLP. The concentrations of Cu in the TCLP leachates of all the hydrochars were highest than other heavy metals, except for Ni in H-180, while the concentrations of Hg and As were not detected at most temperature. The United States Environmental Protection Agency maximum thresholds of determined heavy metal were also illustrated in **Table 3**. No stipulated standards for heavy metals usually are calculated as the drinking water standard multiplied by 100 [55], such as Ni. As shown in **Table 3**, the concentrations of heavy metals in TCLP leachates of the hydrochars were all lower than the US EPA permissible limits, showing that the hydrochars can be considered as non-hazardous materials.

The concentrations of heavy metals in MSW and corresponding hydrochars, such as Cr, Cd, Pb and so on, were determined in **Figure 4**. The results showed that for all determined heavy metals in MSW, Cr had a maximum concentration at a value of 93.29 µg/g and the lowest concentration of heavy metals was Hg (0.15 µg/g). The concentrations of Hg in the hydrochars were still the minimum, while the highest concentration among the heavy metals was Cr at temperature from 160 to 220°C, and As and Zn were the significant dominant metals at 240 and 260°C, respectively. Compared to MSW, the concentrations of Cr, Cd, and Hg in the hydrochars were low, and the other metals exhibited a different trend, which was ascribed to differences in the transformation of heavy metals during HTC. In addition, H-260 had the lowest concentrations of Cr, Pb, and Hg, followed by H-180. As for other heavy metals, except for Cu, the lowest concentrations were observed at H-180. This result indicated that the HTC at 180 and 260°C were a promising method to reduce the content of heavy metals in the hydrochar obtained from MSW.

Heavy metals cannot be destroyed or formed and be just transferred from biomass to waste during HTC. In order to determine the transformation of heavy

Metal	Sample							
	Cr	Cd	Pb	Hg	As	Zn	Ni	Cu
H-160	0.21	0.07	0.81	—	0.31	2.93	0.66	0.22
H-180	0.35	0.24	0.06	—	0.09	1.30	1.46	0.13
H-200	0.30	0.25	0.24	—	—	1.70	0.50	0.40
H-220	0.41	0.35	0.35	—	—	3.49	1.99	0.69
H-240	0.31	0.34	0.06	—	—	3.44	1.63	0.45
H-260	0.12	0.32	0.24	—	—	1.37	0.29	0.64
EPA limit	5.00	1.00	5.00	0.20	5.00	25.00	2.00	100.00

—, not detected.

Table 3.

The concentrations (µg/g) of heavy metals in TCLP leachates of the hydrochars.

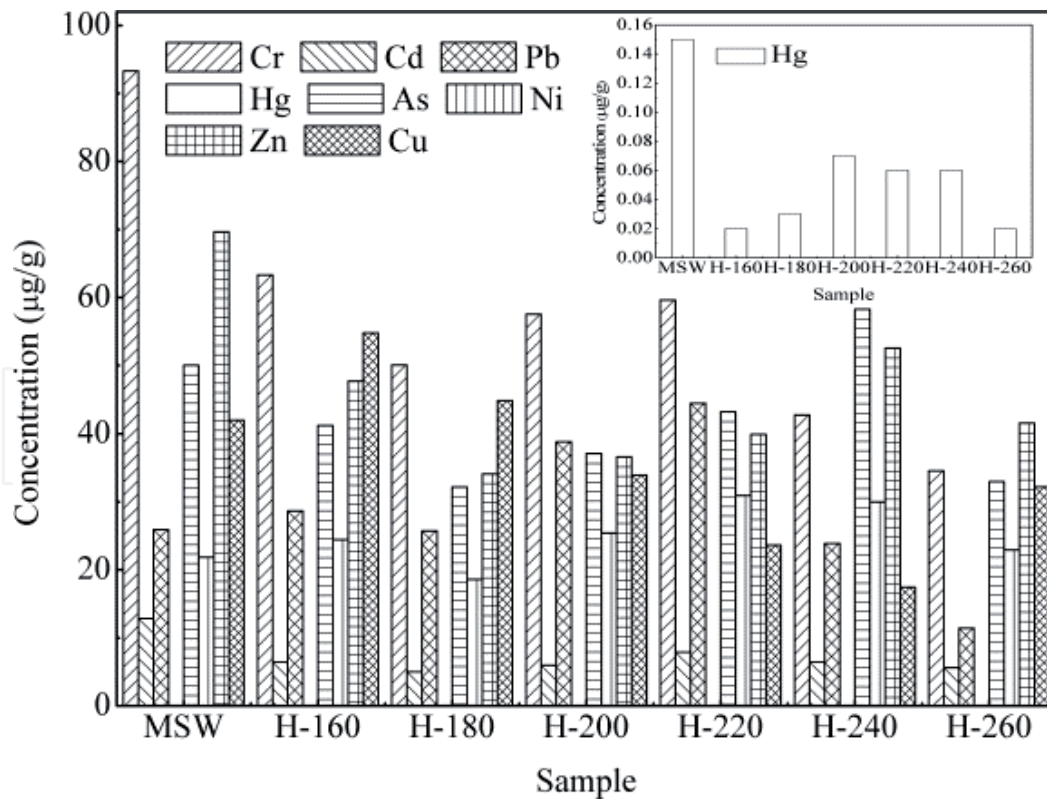


Figure 4.
 The concentrations ($\mu\text{g/g}$) of metals in MSW and corresponding hydrochars.

Metal	Sample					
	H-160	H-180	H-200	H-220	H-240	H-260
Cr	49.14	30.94	31.74	31.94	21.94	13.96
Cd	36.43	22.46	24.33	30.55	24.06	16.46
Pb	80.33	57.32	78.65	85.05	44.30	16.63
Hg	10.45	9.65	24.54	21.49	18.42	6.52
As	59.67	37.02	38.79	42.78	55.77	24.75
Ni	81.13	49.16	60.89	70.20	65.84	39.61
Zn	49.81	28.23	27.51	28.43	36.16	22.48
Cu	94.57	61.65	42.33	27.90	19.90	28.82

Table 4.
 The retention rates (%) of heavy metals in the hydrochars at different hydrothermal temperatures.

metals during HTC, the retention rate was determined. The retention rate of individual metal is defined as the percentages of that metal content in the hydrochar over that in the raw material [20]. **Table 4** illustrated the retention rates of heavy metals in the hydrochars at different temperatures. It is observed that Cu exhibited the highest retention rates in H-160 and H-180 at the percentage of 94.57 and 61.65%, respectively. The highest retention rates in H-200 and H-240 were for Pb. As for H-240 and H-260, significant retention rates of Ni were observed. The lowest retention rates in the samples were for Hg at most temperatures, indicating that compared to other determined heavy metals, Hg in MSW was easily transferred and removed during HTC due to the easy volatility of Hg. With respect to the effect of hydrothermal temperature, a quick decrease of retention rate of Cu were observed at temperature from 160 to 240°C and then slightly increased. As for other heavy

metals, the decreases in retention rates were accompanied by an increase in temperature from 160 to 180°C. When the temperature was in the range of 180–220°C, the retention rates increased, while the decreased trend with further increasing temperature was observed except for Hg from 200 to 260°C and Zn and As from 240 to 260°C. This can be explained by the inherent properties and specific chemical forms of heavy metals in MSW.

5. The formation and transformation of PAHs during HTC of MSW

Figure 5 summarized the concentrations of total free PAHs in MSW and corresponding hydrochars. In general, the concentration of PAHs in MSW was 2181.16 µg/kg. The concentrations of PAHs in the hydrochars were in the range of 1298.71–177698.20 µg/kg, which were much higher than that in MSW, especially at high temperature, except for H-160. The experimental results showed that the free PAHs in the hydrochars are not only obtained from MSW, but there also other ways to produce PAHs.

Considering the effect of hydrothermal temperature, the concentrations of PAHs increased with the increase of temperature from 160 to 240°C and conversely decreased when the temperature continued to increase. The competitive decomposition and formation of PAHs during HTC are responsible for the variation of PAH concentrations in the samples. At temperature from 160 to 240°C, the formation of PAHs was the dominant reaction, which promoted the increase of PAHs. The dehydration, decarboxylation, and condensation reactions occurred during the HTC process and became more intensive with the increasing hydrothermal temperature, resulting in the higher degree of coalification and the formation of amorphous hydrochar [56]. The amorphous hydrochar, containing aliphatics, aromatic compounds, and so on, has been proved to cause the increased PAH concentrations [46]. Furthermore, the free radicals like •OH produced from the decomposition of water or the coalification of MSW promote the formation of PAHs [50]. Additionally, the formations of PAHs are endothermic reactions indicating that the formation of PAHs can be promoted by the increasing temperature. In summary, the formation of PAHs was the dominant reaction at hydrothermal temperature from 160 to 240°C. Conversely, the concentrations of PAHs reduced with further increasing temperature due to the breakdown of structure of the hydrochar. As evidenced in **Figure 4**, the amount of microspheres increased with the temperature from 160 to 240°C, indicating that more produced and higher observed. However, the microspheres are damaged at 260°C, showing that the porous structure collapsed. It is reported that the porous structure of the hydrochars played an important role in absorbing the sugars, furfurals, and so on due to the abundant potential active sites, resulting in increased PAH concentrations [57]. As a result, the porous structure of H-260 is damaged leading to the decrease of PAH concentrations. It is interesting to note that the concentrations of metals also have the effect of the formation of PAHs. For example, Zn promoted the formation of PAHs, and Cu was not favorable for the formation of PAHs, which was consistent with the result in the present study [58]. In detail, the highest concentration of PAHs was obtained at 240°C, which the lowest concentration of Cu and the highest concentration of Zn were observed in H-240. It can be seen that PAHs can be transferred and formed during HTC, which is different from heavy metals, and the transformation and the formation of PAHs are affected by the structure and metal concentration.

The concentrations of 16 individual PAHs in MSW and corresponding hydrochars were illustrated in **Table 5**. The results showed that the concentration of BaA in MSW was 938.01 µg/kg at a value of 43.01% of the total PAHs, followed by Phe

(436.41 $\mu\text{g}/\text{kg}$) and Fla (199.40 $\mu\text{g}/\text{kg}$). Meanwhile, Nap, Flu, and Phe in the hydrochars, except for H-260, accounted for the majority of total PAHs. As for H-260, Flu, Phe, and Chr were the dominant individual PAHs at values of 25.50, 27.79, and 18.59%, respectively. It was thought that the molecular sizes of dominant PAHs in the hydrochars were lower than that in MSW.

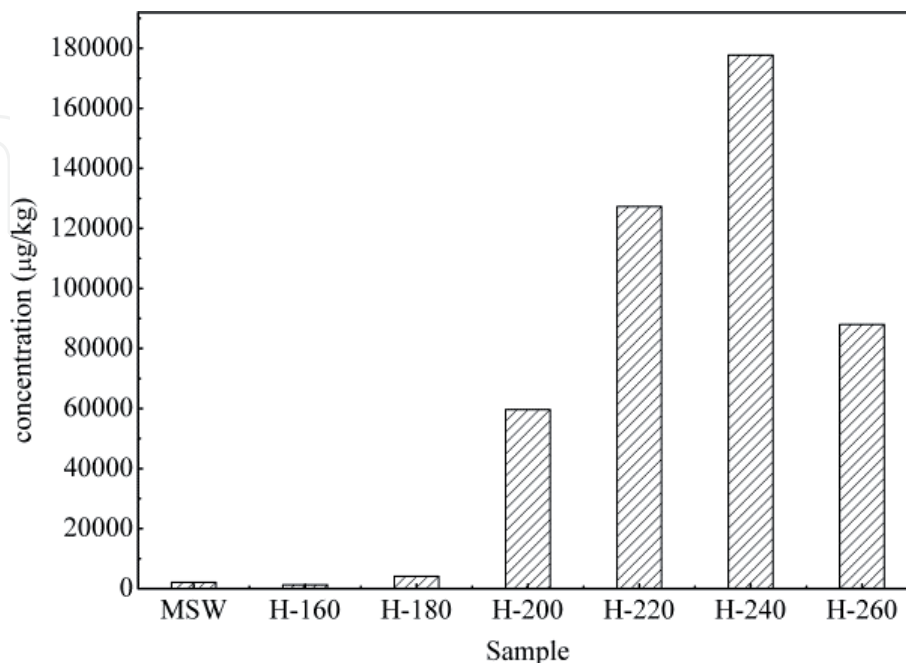


Figure 5.
 The concentrations ($\mu\text{g}/\text{kg}$) of total free PAHs in MSW and corresponding hydrochars.

PAHs	Sample						
	MSW	H-160	H-180	H-200	H-220	H-240	H-260
Nap	101.91	319.13	740.34	11561.17	38824.40	46665.05	9504.29
Acy	2.27	1.75	2.45	3.50	43.27	63.24	49.33
Ace	10.36	10.96	30.17	245.37	618.05	815.80	533.56
Flu	118.65	580.92	1373.72	25429.68	38284.80	45850.40	22438.64
Phe	436.41	272.21	1605.30	14813.56	31264.00	45048.85	24455.65
Ant	28.45	11.85	32.62	340.73	1404.53	2646.07	4125.61
Fla	199.40	30.09	116.01	322.66	1024.09	2082.74	1709.28
Pyr	156.49	21.09	83.71	187.06	377.09	794.50	647.95
BaA	938.01	3.40	13.10	634.05	1653.12	3809.17	2133.97
Chr	83.95	16.68	164.94	5834.41	12674.34	25374.60	16356.79
BbF	36.04	2.48	2.93	96.96	453.23	2086.83	2414.22
BkF	19.19	1.14	6.13	67.24	247.10	613.68	984.55
BaP	9.97	2.06	2.06	49.12	114.45	364.21	669.98
IcP	16.07	1.82	2.14	6.63	11.85	150.01	183.71
DaA	10.51	1.39	3.59	55.84	183.85	717.15	975.35
BgP	13.48	1.74	3.09	22.88	155.25	615.88	799.38

Table 5.
 The concentration ($\mu\text{g}/\text{kg}$) of 16 individual PAHs in MSW and corresponding hydrochars.

In order to investigate the change of molecular size during HTC process, the 16 individual PAHs are classified by ring number according to **Table 1**. The result was illustrated in **Figure 6**. As can be seen from **Figure 6a**, in MSW, the two-, three-, four-, five- and six-ring PAHs comprised about 4.67, 27.33, 63.17, 3.47, and 1.35% of total PAHs, respectively, indicating that four-ring PAHs were the most prevalent in MSW. As for the hydrochars, the concentrations of three-ring PAHs exhibited a maximum in the range of 53.14–72.79% of the hydrochars obtained at temperature from 160 to 260°C. Additionally, the concentrations of two-, three-, and four-ring PAHs in the hydrochars increased with an increase of hydrothermal temperature, showed a maximum at 240°C, and decreased with further increasing temperature. However, an increase in the concentrations of five- and six-ring PAHs in the hydrochars was accompanied by an increase in the temperature. **Figure 6b** showed the effect of hydrothermal temperature on the molecular weight of PAHs in MSW and

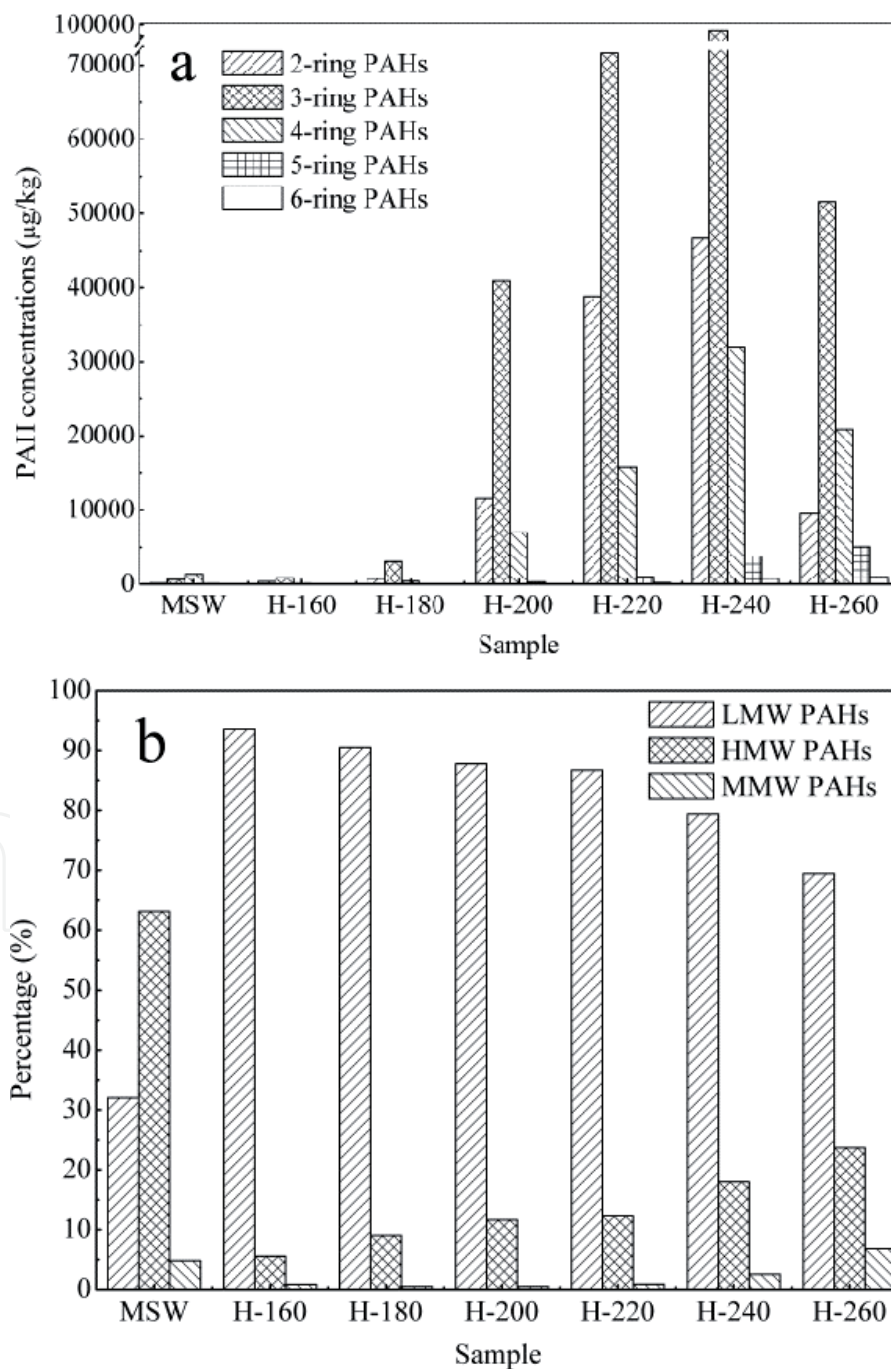


Figure 6. The ring number (a) and percentages of LMW, MMW, and HMW PAHs (b) in MSW and corresponding hydrochars.

corresponding hydrochars. In detail, PAHs contained low molecular weight PAHs (LMW PAHs, two- and three-ring PAHs), middle molecular weight PAHs (MMW PAHs, four-ring PAHs), and high molecular weight PAHs (HMW PAHs, five- and six-ring PAHs) [39]. Considering the MSW, significant percentage of MMW PAHs was observed, at a value of 63.14% of total PAHs, while the percentages of LMW and HMW PAHs were 32.04% and 4.82%, respectively. As for the hydrochars, the LMW PAHs had maximum percentages of 69.45–93.59% of total PAHs, which reduced with an increase of hydrothermal temperature. Compared to LMW PAHs, however, the MMW PAHs and HMW PAHs (in the range of 5.57–23.69% and 0.47–6.85%, respectively) exhibited a different trend with hydrothermal temperature. The above results confirmed that the dominant PAHs in MSW were higher than that in the hydrochar.

The higher ring number and molecular weight of PAHs are expected to have higher toxicity [58]. In order to analyze the toxicity of PAHs in MSW and corresponding hydrochars, the TEQ value of 16 priority PAHs is used according to the following equation [50]:

$$\text{TEQ} = \sum(\text{TEF}_i \times C_i) \quad (1)$$

where TEF values of the 16 individual PAHs are shown in **Table 1**. C represents the concentration of 16 individual PAHs in the hydrochars obtained at different hydrothermal temperatures. *i* denotes each 16 individual PAHs.

According to Eq. (1), the TEQ values of MSW and corresponding hydrochars are shown in **Figure 7**. Considering the effect of the hydrothermal temperature (160–260°C), significant increase in TEQ values of the hydrochars from 5.87 µg TEQ/kg to 2489.13 µg TEQ/kg occurred. The TEQ value of MSW (123.7 µg TEQ/kg) was at least eight times higher than that of H-160 and H-180 and lower than that of other hydrochars. It was interesting to note that the total PAHs of MSW was lower and the TEQ was higher than that of H-180. It is indicating that, considering the concentration and toxicity of PAHs, 160 and 180°C are the suitable hydrothermal temperatures to reduce the concentrations and toxicity of PAHs in MSW.

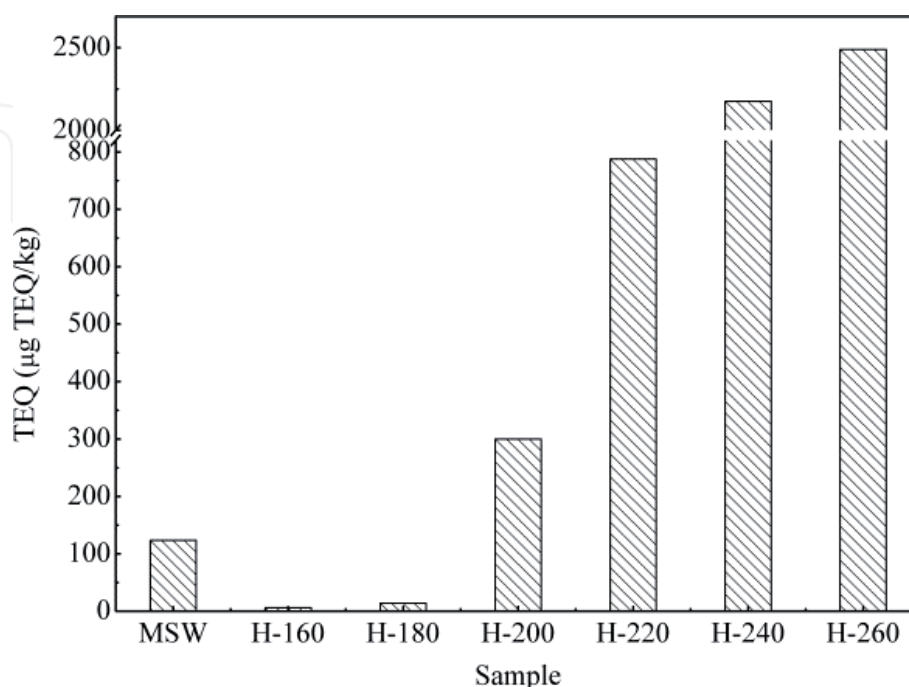


Figure 7.
The TEQ values (µg TEQ/kg) of MSW and corresponding hydrochars.

6. Challenges

Commercialization of HTC of MSW for biofuel production should overcome the following major challenges:

- HTC requires a large heat input for its carbonization reactions and for maintenance of its moderately high reaction temperature. This heat requirement greatly reduces energy conversion efficiency and greatly increases its capital cost.
- The pretreatment and feeding of wet MSW, which is fibrous and widely varying in composition, is another major challenge.
- Separation of product may require the addition of energy consumption, and this can greatly increase the system's cost and reduce its overall energy efficiency.

Further research is required to address this important challenge. A final problem that might inhibit commercialization of HTC of MSW is the corrosion of the reactor wall.

7. Conclusions

In this chapter, the formation and transformation of heavy metals and free PAHs during HTC of MSW were analyzed through determining the concentrations of heavy metals and free PAHs in MSW and corresponding hydrochars. The results showed that with the increasing hydrothermal temperature, the hydrochar yield decreased in the range of 37.68–70.37%. But HTC can homogenize the MSW and increase carbon content and HHV, especially at temperature above 160°C. As for the heavy metal, the concentrations of heavy metals in TCLP leachates of the hydrochars were all lower than the US EPA permissible limits. Compared to MSW, the concentrations of Cr, Cd, Hg, and Zn were low, while Pb, As, Ni, and Cu in the hydrochars exhibited a different trend. The PAH concentrations in MSW was 2181.16 µg/kg, which were much lower than that in corresponding hydrochars, except for H-160. The TEQ values were in the order H-260 > H-240 > H-220 > H-200 > MSW > H-180 > H-160. Considering the fuel properties and the contentions of heavy metal and PAHs, the hydrochar obtained at 180°C is a promising alternative solid fuel with high fuel property and environmentally friendly characteristic.

Acknowledgements

The authors are grateful for the financial support from Zhengang Liu from the “100 Talents” Program of the Chinese Academy of Sciences.

Conflict of interests

The authors declare no competing financial interest.

IntechOpen

Author details

Wentao Jiao^{1,2}, Nana Peng^{1,3} and Zhengang Liu^{1,2*}

1 Research Center for Eco-Environmental Sciences, Chinese Academy of Sciences, Beijing, China

2 University of Chinese Academy of Sciences, Beijing, China

3 College of Environmental Science and Engineering, Beijing Forestry University, Beijing, China

*Address all correspondence to: zgliu@rcees.ac.cn

IntechOpen

© 2020 The Author(s). Licensee IntechOpen. This chapter is distributed under the terms of the Creative Commons Attribution License (<http://creativecommons.org/licenses/by/3.0>), which permits unrestricted use, distribution, and reproduction in any medium, provided the original work is properly cited. 

References

- [1] Tozlu A, Özahi E, Abuşoğlu A. Waste to energy technologies for municipal solid waste management in Gaziantep. *Renewable and Sustainable Energy Reviews*. 2016;**54**:809-815. DOI: 10.1016/j.rser.2015.10.097
- [2] Kulkarni B. Environmental sustainability assessment of land disposal of municipal solid waste generated in Indian cities—A review. *Environmental Development*. 2020;**33**:100490. DOI: 10.1016/j.envdev.2019.100490
- [3] Zheng L, Song J, Li C, Gao Y, Geng P, Qu B, et al. Preferential policies promote municipal solid waste (MSW) to energy in China: Current status and prospects. *Renewable and Sustainable Energy Reviews*. 2014;**36**:135-148. DOI: 10.1016/j.rser.2014.04.049
- [4] Chen P, Xie Q, Addy M, Zhou W, Liu Y, Wang Y, et al. Utilization of municipal solid and liquid wastes for bioenergy and bioproducts production. *Bioresource Technology*. 2016;**215**:163-172. DOI: 10.1016/j.apenergy.2016.06.148
- [5] National Bureau of Statistics of the people's Republic of China. Available from: http://www.stats.gov.cn/zjtj/ztsj/hjtjzl/2014/201609/t20160918_1400854.html
- [6] Hoornweg D, Bhada-Tata P, Kennedy C. Environment waste production must peak this century. *Nature*. 2013;**502**:615-617. DOI: 10.1038/502615a
- [7] Gupta D, Mahajani SM, Garg A. Effect of hydrothermal carbonization as pretreatment on energy recovery from food and paper wastes. *Bioresource Technology*. 2019;**285**:121329. DOI: 10.1016/j.biortech.2019.121329
- [8] Li Y, Zhao X, Li Y, Li X. Waste incineration industry and development policies in China. *Waste Management*. 2015;**46**:234-241. DOI: 10.1016/j.wasman.2015.08.008
- [9] Maqhuzu A, Yoshikawa K, Takahashi F. Stochastic economic analysis of coal-alternative fuel production from municipal solid wastes employing hydrothermal carbonization in Zimbabwe. *Sciences of The Total Environment*. 2019;**23**:135337. DOI: 10.1016/j.scitotenv.2019.135337
- [10] Peng N, Liu Z, Liu T, Gai C. Emissions of polycyclic aromatic hydrocarbons (PAHs) during hydrothermally treated municipal solid waste combustion for energy generation. *Applied Energy*. 2016;**184**:396-403. DOI: 10.1016/j.apenergy.2016.10.028
- [11] Fonts I, Gea G, Azuara M, Ábrego J, Arauzo J. Sewage sludge pyrolysis for liquid production: A review. *Renewable and Sustainable Energy Reviews*. 2012;**16**:2781-2805. DOI: 10.1016/j.rser.2012.02.070
- [12] Yang W, Wang H, Zhang M, Zhu J, Zhou J, Wu S. Fuel properties and combustion kinetics of hydrochar prepared by hydrothermal carbonization of bamboo. *Bioresource Technology*. 2016;**205**:199-204. DOI: 10.1016/j.biortech.2016.01.068
- [13] Basso D, Patuzzi F, Castello D, Baratieri M, Rada EC, Weiss-Hortala E, et al. Agro-industrial waste to solid biofuel through hydrothermal carbonization. *Waste Management*. 2016;**47**(Part A):114-121. DOI: 10.1016/j.wasman.2015.05.013
- [14] Kambo HS, Dutta A. Comparative evaluation of torrefaction and hydrothermal carbonization of lignocellulosic biomass for the production of solid biofuel. *Energy Conversion and Management*.

2015;**105**:746-755. DOI: 10.1016/j.enconman.2015.08.031

[15] Tekin K, Karagöz S, Bektaş S. A review of hydrothermal biomass processing. *Renewable and Sustainable Energy Reviews*. 2014;**40**:673-687. DOI: 10.1016/j.rser.2014.07.216

[16] Akiya N, Savage PE. Roles of water for chemical reactions in high-temperature water. *ChemInform*. 2002;**33**:293-293. DOI: 10.1002/chin.200243293

[17] Benavente V, Calabuig E, Fullana A. Upgrading of moist agro-industrial wastes by hydrothermal carbonization. *Journal of Analytical and Applied Pyrolysis*. 2015;**113**:89-98. DOI: 10.1016/j.jaap.2014.11.004

[18] Mäkelä M, Benavente V, Fullana A. Hydrothermal carbonization of lignocellulosic biomass: Effect of process conditions on hydrochar properties. *Applied Energy*. 2015;**155**:576-584. DOI: 10.1016/j.apenergy.2015.06.022

[19] Xiao L, Shi Z, Xu F, Sun R. Hydrothermal carbonization of lignocellulosic biomass. *Bioresource Technology*. 2012;**118**:619-623. DOI: 10.1016/j.biortech.2012.05.060

[20] Liu Z, Balasubramanian R. Upgrading of waste biomass by hydrothermal carbonization HTC and low temperature pyrolysis LTP: A comparative evaluation. *Applied Energy*. 2014;**114**:857-864. DOI: 10.1016/j.apenergy.2013.06.027

[21] Berge ND, Ro KS, Mao J, FloraJoseph RV, Chappell MA, Bae S. Hydrothermal carbonization of municipal waste streams. *Environmental Science & Technology*. 2011;**45**:5696-5703. DOI: 10.1021/es2004528

[22] Funke A, Ziegler F. Hydrothermal carbonization of biomass: A

summary and discussion of chemical mechanisms for process engineering. *Biofuels, Bioproducts and Biorefining*. 2010;**4**:160-177. DOI: 10.1002/bbb.198

[23] Titirici MM, Thomas A, Antonietti M. Back in the black: Hydrothermal carbonization of plant material as an efficient chemical process to treat the CO₂ problem? *New Journal of Chemistry*. 2007;**31**:787-789. DOI: 10.1039/B616045J

[24] Bobleter O. Hydrothermal degradation of polymers derived from plants. *Progress in Polymer Science*. 1994;**19**:797-841. DOI: 10.1016/0079-6700(94)90033-7

[25] Hoekman SK, Broch A, Robbins C. Hydrothermal carbonization HTC of lignocellulosic biomass. *Energy & Fuels*. 2011;**25**:1802-1810. DOI: 10.1021/ef101745n

[26] Reza MT, Rottler E, Herklotz L, Wirth B. Hydrothermal carbonization HTC of wheat straw: Influence of feedwater pH prepared by acetic acid and potassium hydroxide. *Bioresource Technology*. 2015;**182**:336-344. DOI: 10.1016/j.biortech.2015.02.024

[27] Huff MD, Kumar S, Lee JW. Comparative analysis of pinewood, peanut shell, and bamboo biomass derived biochars produced via hydrothermal conversion and pyrolysis. *Journal of Environmental Management*. 2014;**146**:303-308. DOI: 10.1016/j.jenvman.2014.07.016

[28] Sabio E, Álvarez-Murillo A, Román S, Ledesma B. Conversion of tomato-peel waste into solid fuel by hydrothermal carbonization: Influence of the processing variables. *Waste Management*. 2016;**47**(Part A):122-132. DOI: 10.1016/j.wasman.2015.04.016

[29] Dai L, Tan F, Wu B, He M, Wang W, Tang X, et al. Immobilization of phosphorus in cow manure during

- hydrothermal carbonization. *Journal of Environmental Management*. 2015;**157**:49-53. DOI: 10.1016/j.jenvman.2015.04.009
- [30] Lu Y, Levine RB, Savage PE. Fatty acids for nutraceuticals and biofuels from hydrothermal carbonization of microalgae. *Industrial & Engineering Chemistry Research*. 2015;**54**:4066-4071. DOI: 10.1021/ie503448u
- [31] Burguete P, Corma A, Hitzl M, Modrego R, Ponce E, Renz M. Fuel and chemicals from wet lignocellulosic biomass waste streams by hydrothermal carbonization. *Green Chemistry*. 2016;**18**:1051-1060. DOI: 10.1039/C5GC02296G
- [32] Zuo X, Liu Z, Chen M. Effect of H₂O₂ concentrations on copper removal using the modified hydrothermal biochar. *Bioresource Technology*. 2016;**207**:262-267. DOI: 10.1016/j.biortech.2016.02.032
- [33] Lynam JG, Coronella CJ, Yan W, Reza MT, Vasquez VR. Acetic acid and lithium chloride effects on hydrothermal carbonization of lignocellulosic biomass. *Bioresource Technology*. 2011;**102**:6192-6199. DOI: 10.1016/j.biortech.2011.02.035
- [34] Reza MT, Lynam JG, Uddin MH, Coronella CJ. Hydrothermal carbonization: Fate of inorganics. *Biomass and Bioenergy*. 2013;**49**:86-94. DOI: 10.1016/j.biombioe.2012.12.004
- [35] Peng N, Li Y, Liu T, Lang Q, Gai C, Liu Z. Polycyclic aromatic hydrocarbons and toxic heavy metals in municipal solid waste and corresponding hydrochars. *Energy & Fuels*. 2017;**31**:1665-1671. DOI: 10.1021/acs.energyfuels.6b02964
- [36] Košnář Z, Mercl F, Perná I, Tlustoš P. Investigation of polycyclic aromatic hydrocarbon content in fly ash and bottom ash of biomass incineration plants in relation to the operating temperature and unburned carbon content. *Science of the Total Environment*. 2016;**563-564**:53-61. DOI: 10.1016/j.scitotenv.2016.04.059
- [37] Perera FP, Tang D, Wang S, Vishnevetsky J, Zhang B, Diaz D, et al. Prenatal polycyclic aromatic hydrocarbon PAH exposure and child behavior at age 6-7 years. *Environmental Health Perspectives*. 2012;**120**:921-926. DOI: 10.1289/ehp.1104315
- [38] Alves CA, Vicente AMP, Gomes J, Nunes T, Duarte M, Bandowe BAM. Polycyclic aromatic hydrocarbons PAHs and their derivatives oxygenated-PAHs, nitrated-PAHs and azaarenes in size-fractionated particles emitted in an urban road tunnel. *Atmospheric Research*. 2016;**180**:128-137. DOI: 10.1016/j.atmosres.2016.05.013
- [39] Peng N, Li Y, Liu Z, Liu T, Gai C. Emission, distribution and toxicity of polycyclic aromatic hydrocarbons PAHs during municipal solid waste MSW and coal co-combustion. *Science of the Total Environment*. 2016;**565**:1201-1207. DOI: 10.1016/j.scitotenv.2016.05.188
- [40] Chen Y, Zhi G, Feng Y, Fu J, Feng J, Sheng G, et al. Measurements of emission factors for primary carbonaceous particles from residential raw-coal combustion in China. *Geophysical Research Letters*. 2006;**33**:1-4. DOI: 10.1029/2006gl026966
- [41] Rajput P, Sarin MM, Sharma D, Singh D. Atmospheric polycyclic aromatic hydrocarbons and isomer ratios as tracers of biomass burning emissions in Northern India. *Environmental Science and Pollution Research International*. 2014;**21**:5724-5729. DOI: 10.1007/s11356-014-2496-5
- [42] Zhou H, Wu C, Onwudili JA, Meng A, Zhang Y, Williams PT. Influence of process conditions on the formation

of 2-4 ring polycyclic aromatic hydrocarbons from the pyrolysis of polyvinyl chloride. *Fuel Processing Technology*. 2016;**144**:299-304. DOI: 10.1016/j.fuproc.2016.01.013

[43] Dong J, Li F, Xie K. Study on the source of polycyclic aromatic hydrocarbons PAHs during coal pyrolysis by PY-GC-MS. *Journal of Hazardous Materials*. 2012;**243**:80-85. DOI: 10.1016/j.jhazmat.2012.09.073

[44] Verma SK, Masto RE, Gautam S, Choudhury DP, Ram LC, Maiti SK, et al. Investigations on PAHs and trace elements in coal and its combustion residues from a power plant. *Fuel*. 2015;**162**:138-147. DOI: 10.1016/j.fuel.2015.09.005

[45] Shen C, Tang X, Yao J, Shi D, Fang J, Khan MI, et al. Levels and patterns of polycyclic aromatic hydrocarbons and polychlorinated biphenyls in municipal waste incinerator bottom ash in Zhejiang province, China. *Journal of Hazardous Materials*. 2010;**179**:197-202. DOI: 10.1016/j.jhazmat.2010.02.079

[46] Keiluweit M, Kleber M, Sparrow MA, Simoneit BRT, Prah FG. Solvent-extractable polycyclic aromatic hydrocarbons in biochar: Influence of pyrolysis temperature and feedstock. *Environmental Science & Technology*. 2012;**46**:9333-9341. DOI: 10.1021/es302125k

[47] Etoh J, Kawagoe T, Shimaoka T, Watanabe K. Hydrothermal treatment of MSWI bottom ash forming acid-resistant material. *Waste Management*. 2009;**29**:1048-1057. DOI: 10.1016/j.wasman.2008.08.002

[48] US EPA. Tests methods for evaluating solid waste, Physical Chemical Methods. SW-846, Method 1311. Washington, DC: US Environmental Protection Agency; 1992. Available from: <http://>

www.epa.gov/epaoswer/hazwaste/test/pdfs/1311pdf

[49] Liu S, Tao S, Liu W, Liu Y, Dou H, Zhao J, et al. Atmospheric polycyclic aromatic hydrocarbons in North China: A winter-time study. *Environmental Science & Technology*. 2007;**41**:8256-8261. DOI: 10.1021/es0716249

[50] Liu S, Wang C, Zhang S, Liang J, Chen F, Zhao K. Formation and distribution of polycyclic aromatic hydrocarbons PAHs derived from coal seam combustion: A case study of the Ulanqab lignite from Inner Mongolia, northern China. *International Journal of Coal Geology*. 2012;**90-91**:126-134. DOI: 10.1016/j.coal.2011.11.005

[51] Liu Z, Quek A, Hoekman KS, Balasubramanian R. Production of solid biochar fuel from waste biomass by hydrothermal carbonization. *Fuel*. 2013;**103**:943-949. DOI: 10.1016/j.fuel.2012.07.069

[52] Kim D, Lee K, Park KY. Hydrothermal carbonization of anaerobically digested sludge for solid fuel production and energy recovery. *Fuel*. 2014;**130**:120-125. DOI: 10.1016/j.fuel.2014.04.030

[53] Liu Z, Balasubramanian R. Hydrothermal carbonization of waste biomass for energy generation. *Procedia Environmental Sciences*. 2012;**16**:159-166. DOI: 10.1016/j.proenv.2012.10.022

[54] Zhao L, Zhang FS, Chen M, Liu Z, Wu DBJ. Typical pollutants in bottom ashes from a typical medical waste incinerator. *Journal of Hazardous Materials*. 2010;**173**:181-185. DOI: 10.1016/j.jhazmat.2009.08.066

[55] Skodras G, Grammelis P, Prokopidou M, Kakaras E, Sakellaropoulos G. Chemical, leaching and toxicity characteristics of CFB combustion residues. *Fuel*.

2009;**88**:1201-1209. DOI: 10.1016/j.fuel.2007.06.009

[56] Keiluweit M, Nico PS, Johnson MG, Kleber M. Dynamic molecular structure of plant biomass-derived black carbon biochar. *Environmental Science & Technology*. 2010;**44**:1247-1253. DOI: 10.1021/es9031419

[57] Reza MT, Uddin MH, Lynam JG, Coronella CJ. Engineered pellets from dry torrefied and HTC biochar blends. *Biomass and Bioenergy*. 2014;**63**:229-238. DOI: 10.1016/j.biombioe.2014.01.038

[58] Chen Y, Zhao R, Xue J, Li J. Generation and distribution of PAHs in the process of medical waste incineration. *Waste Management*. 2013;**33**:1165-1173. DOI: 10.1016/j.wasman.2013.01.011

IntechOpen